

BOREHOLE IMAGE ANALYSIS AND GEOLOGICAL INTERPRETATION OF SELECTED FEATURES IN WELL DP 27-15 AT DESERT PEAK, NEVADA: PRE-STIMULATION EVALUATION OF AN ENHANCED GEOTHERMAL SYSTEM

K.M. Kovac¹, Susan J. Lutz², Peter S. Drakos³, Joel Byersdorfer⁴, and Ann Robertson-Tait⁵

1 Schlumberger, Data and Consulting Services, Bakersfield, CA 93311

2 TerraTek, A Schlumberger Company, Salt Lake City, UT 84104

3 ORMAT Nevada Inc., Reno NV 89511

4 Schlumberger, Data and Consulting Services, Greenwood Village, CO 80111

5 GeothermEx Inc., Richmond, CA 94806

e-mail:kkovac@slb.com

ABSTRACT

An industry-DOE cost-shared project is underway to evaluate the technical feasibility of developing an Enhanced Geothermal System (EGS) power generation project in Desert Peak (Nevada) geothermal field. As part of pre-stimulation analysis, a non-commercial well (DP 27-15) in the hydrothermal portion of the field has been image-logged to aid in evaluating lithologies and stress and fracture characterization of potential reservoir units as part of a multidisciplinary study. Borehole images, gamma ray, caliper, and cable tension were recorded by Schlumberger's Formation MicroScanner* tool run in the well and compared with geological features identified by petrologic analysis of well cuttings. The wellbore image log obtained from deeper portions of the well (3057.5-5620 ft; ~932-1712 m) has been analyzed. Features identified from these resistivity-contrast generated images include bedding planes, lithologic contacts, foliations, conductive mineral grains, drilling induced fractures, and natural fractures. This paper describes selected geologic features seen on the image logs that may influence the design and success of stimulation activities in the potential reservoir, as part of a multi-disciplinary approach to understanding EGS systems.

INTRODUCTION

Ormat Nevada and the DOE are currently collaborating to explore the possibility of an EGS power-generation project on the eastern side of the Desert Peak, NV geothermal resource. The Ormat Desert Peak 27-15 well was drilled and then logged and analyzed using a multi-disciplinary approach to help evaluate the geothermal potential of the eastern

part of the field, and is the proposed hydraulic stimulation well for the enhanced geothermal systems study (Davatzes and Hickman, 2009; Lutz et al., 2009).

Lithologic, stress, and fracture analysis has been prepared using the Formation MicroScanner* (FMS-4) tool from 3057.5' to 5620' (~932-1712 m). In this paper depth units are listed in feet (English units). The data was processed and interpreted using GeoFrame* software (version 4.0.4.1) by Schlumberger in Bakersfield, CA. In general, the data was fair to good in quality. The guidance package and 4 image pads are 100% operational. However, the large borehole diameter coupled with poor pad contact on one of the four pads resulted in limited borehole coverage of about 21%. Metamorphosed intrusives, metasedimentary rocks, and tuffaceous intervals were encountered. Detailed petrologic and petrographic studies were conducted by the Energy and Geoscience Institute. Lithology/petrology, vein mineral paragenesis, and clay and alteration mineralogy were determined based on thin section, cuttings, and x-ray diffraction analysis. In this paper the petrologic and petrographic study results are coupled with the resistivity image log results.

GEOLOGIC SETTING

The Hot Springs Mountains, located about 55 miles ESE of Reno, NV, rise to a maximum elevation of about 5,400 feet (1,646 m) above sea level and are veneered by Quaternary and Tertiary volcanic and metasedimentary rocks (Figure 1) (Lutz et al., 2009). Adjacent ranges consist of various Mesozoic sedimentary, volcanic and granitic rocks overlain by Tertiary volcanic formations similar to those found in the Hot Springs Mountains (Willden and Speed, 1974; Benoit and others, 1982). Several faults are

*All asterisked items are property of Schlumberger Technology Corporation.

located within the area including the Rhyolite Ridge Fault, the Desert Queen Fault, and the Desert Peak Fault. Extensive drilling in the Desert Peak geothermal area has shown that the northern Hot Springs Mountains are underlain by Mesozoic metamorphic and granitic rocks (Benoit and others, 1982; Lutz et al., 2003; Robertson-Tait et al., 2004). These crystalline rocks are the subject of the current EGS study. Well 27-15, the well proposed for hydraulic stimulation and creation of an enhanced geothermal system, is located north of the horst block in downthrown basement rocks (Lutz et al., 2009).

ELECTRICAL BOREHOLE IMAGE LOGGING

Schlumberger’s Formation MicroScanner* (FMS) tool was used to log a resistivity-contrast generated borehole image log of the study interval in DP 27-15. This older generation tool provides less borehole

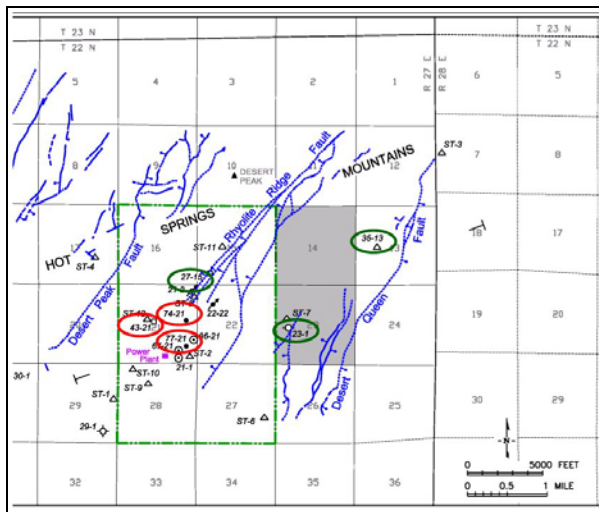


Figure 1: Area map of the Desert Peak geothermal area showing the location of study well 27-15 circled in green near the Rhyolite Ridge Fault.

coverage than the newer Formation MicroImager* tool (4 pad sensors as opposed to 4 pad and 4 flap sensors), but is more robust to the high borehole temperatures typically found in geothermal wells (up to 350 degrees unflashed). Caliper, gamma ray, cable tension, and resistivity measurements were logged. The images generated were processed and interpreted using GeoFrame* version 4.041. The image quality is fair to good on three of four pad sensors. In the images shown, darker colored zones are relatively electrically conductive, while brighter zones or features are relatively electrically resistive. Due to the large borehole size and reduced visibility from one pad, borehole coverage was about 18%. While this coverage is sufficient to identify foliations, continuous natural fractures, hydrothermal breccias, and other features, the reduced borehole coverage

certainly can obscure such discontinuous features as drilling induced fractures, partial borehole washouts, and partial or lithologically-bound natural fractures. The images were processed using two different methods: ‘dynamic’ that enhances contrast over each 2 ft interval; and ‘static’ that scales contrast based on variety found over the entire logged interval.

LITHOLOGIC DESCRIPTION OF MAJOR UNITS IN THE LOGGED INTERVAL

The imaged interval of well 27-15 consists of three major parts. From 3057.5 – 3300 ft measured depth the altered Tertiary rhyolitic tuffs interval is encountered. Below this, the pre-Tertiary Unit 1, consisting largely of weakly metamorphosed hematitic and dolomitic mudstones occurs between 3300 and 4800 feet measured depth (Lutz et al., 2009). Pre-Tertiary Unit 2 from 4800 to 5620 ft includes strongly propylitically-altered and metamorphosed diorites, foliated phyllites and hornfels.

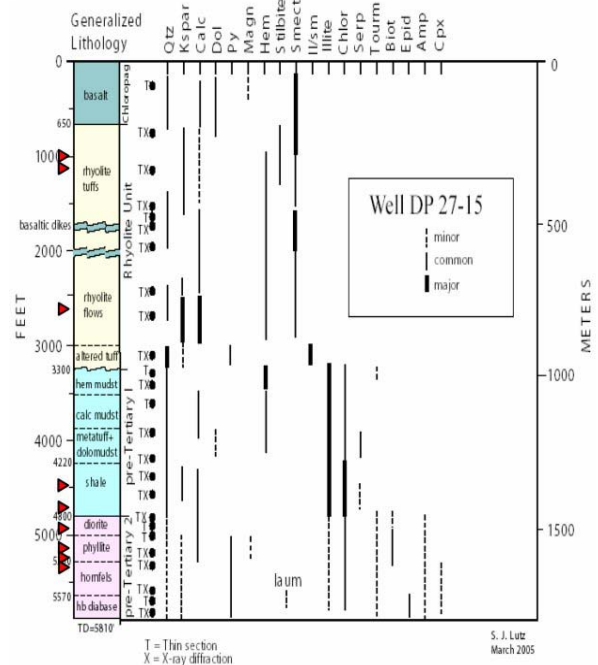


Figure 2: Lithologic column and distribution of secondary and hydrothermal alteration minerals in Well 27-15 (from Lutz, 2005). Red arrows show the locations of lost circulation zones.

In the FMI images, the Tertiary rhyolitic tuff interval appears relatively conductive. Gamma ray readings in the tuff are much higher than in the underlying pre-Tertiary Unit 1 metasedimentary sequence. The average gamma ray reading in the tuffs is 184 gAPI vs. average readings of 60.5 gAPI in the metasedimentary rocks, and 84.0 gAPI in the pre-

Tertiary Unit 2 below. In the upper portion of the tuffaceous interval, the foliations are more clearly defined and some degree of both some drilling induced and natural fracturing is present (Figure 3). However, in the lower portion of this zone beginning at around 3190 ft, the foliation planes appear less distinct and fairly warped (non-planar) over most of the zone. Also, both the drilling induced and natural fracturing present above seems to largely disappear in this interval.

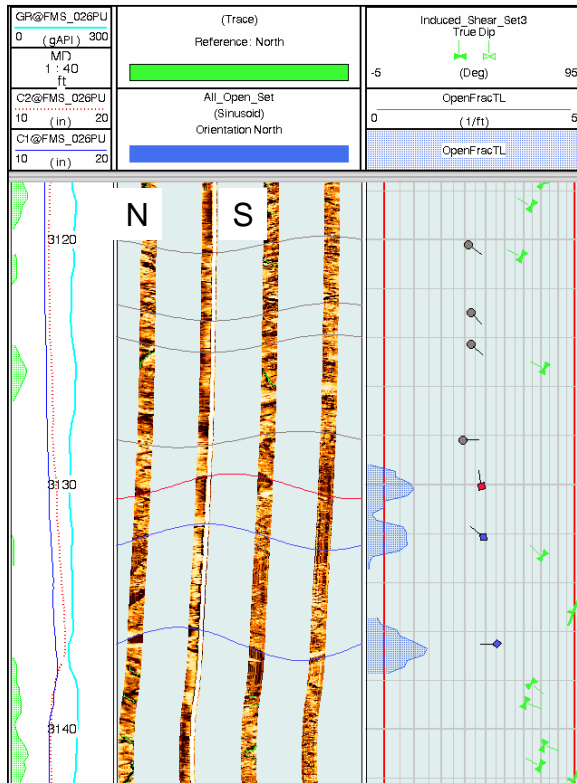


Figure 3: FMS* image from the Tertiary unit (~3120-3142 ft). The image is shown with dynamic normalization to enhance detail, and is shown 'unwrapped', with the left side of the image oriented to north, the middle of the figure is south, and the right side of the figure north again. The leftmost column displays caliper and gamma ray information. The right-most column lists dip magnitude information with the left red line being 0° dip magnitude and the right being 90°. The orientation of the small line on the dip symbols indicates their azimuth orientation. The blue and red marked features represent natural fractures, and the green features represent drilling induced fractures. Note the irregular texture in this tuffaceous interval.

The 3300 - 4800 ft interval (pre-Tertiary 1 unit) consists mostly of weakly metamorphosed, hematitic

and calcareous/dolomitic mudstones and shales (Figure 2) (Lutz et al., 2009). XRD and petrographic studies indicate for the most part the mudstones are only weakly foliated. These rocks consist of mostly quartz, muscovite, illite, and chlorite with minor hematite and pyrite; there are traces of andalusite and some of the cuttings are more strongly foliated. In the FMI images the bedding planes in the hematitic mudstones are about ten degrees in dip magnitude and generally dipping WNW. Below this (~3500-3800'), bedding planes in the calcareous/dolomitic mudstones are in general dipping to the southwest and also about 10 degrees dip magnitude in average. Several possible fault zones are present in the metasedimentary interval. These are suggested on the image logs by zones of abrupt changes in bedding plane orientations and are sometimes coupled with increased abundance of natural fracturing. An example would be at 4544- 4556 ft. A moderate degree of drilling induced fracturing is present throughout most of the metasedimentary sequence.

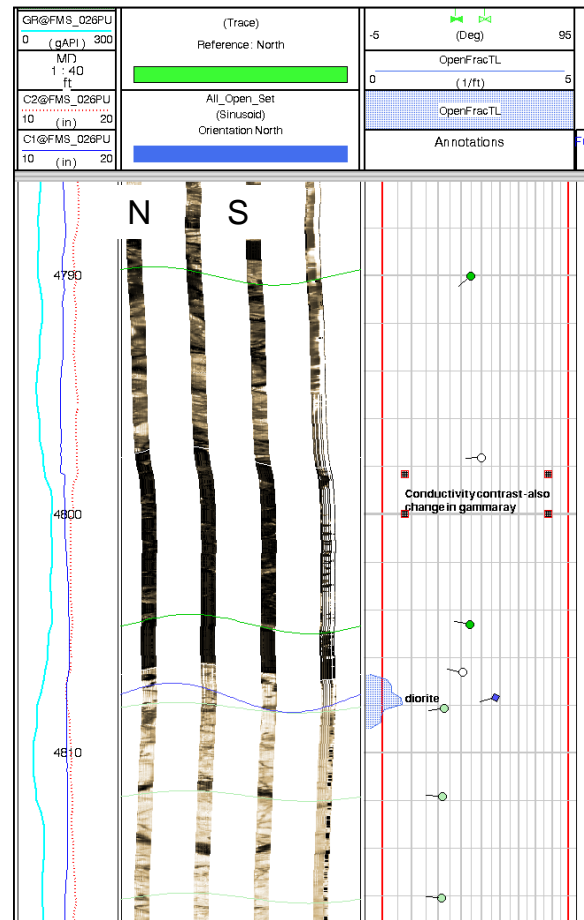


Figure 4: FMS* image from the Tertiary unit – pre-Tertiary unit 1 boundary (~4786-4817 ft shown). In this figure, the static image is shown to highlight the resistivity contrast between the two units). Other log conventions are as described in Fig. 3.

The pre-Tertiary Unit 2 zone beginning at ~4800 ft consists of metamorphosed intrusive rocks, namely diorite, phyllite, hornfels, and hornblende diabase. At 4807 ft MD on the log, a sharp resistivity contrast is seen between the relatively conductive shales above and relatively resistive diorite below (Figure 4). The diorite displays relatively distinct foliation bands that vary in orientation. Natural and drilling induced fractures are present. The diorite-phyllite contact is again marked by a sharp resistivity contrast at 5041 ft MD on the log. The phyllite has a clearly defined metamorphic texture. It has natural fracturing but is generally lacking in drilling induced fractures. The phyllite displays variety in its foliation plane orientations, suggesting several fault or microfault zones. The zone from 5080 – 5110 ft is an example, showing a wide variety in foliation plane orientations and increased intensity of natural fracturing (Figure 5).

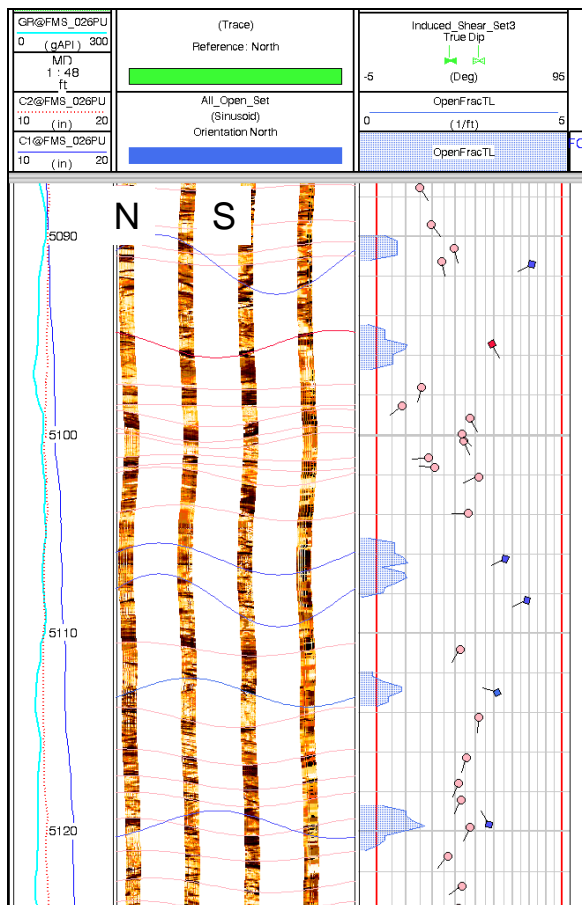


Figure 5: FMS* dynamic image of the phyllite (~5087 -5126' shown here). Figure conventions are as described in Figure 3. Note the irregularity in orientation of the foliation planes, suggesting possible fault zone. Also, note increased intensity in natural fractures in this interval.

Below the phyllite, the hornfels (5300- 5570 ft) displays a distinctive fabric with the more mafic mineral bands consisting of biotite and hornblende appearing as sharp, dark, conductive bands on the images and very regular foliation planes dipping down to the SW (average dip magnitude: 35.5°, average dip azimuth: 209.6° (Figure 6).

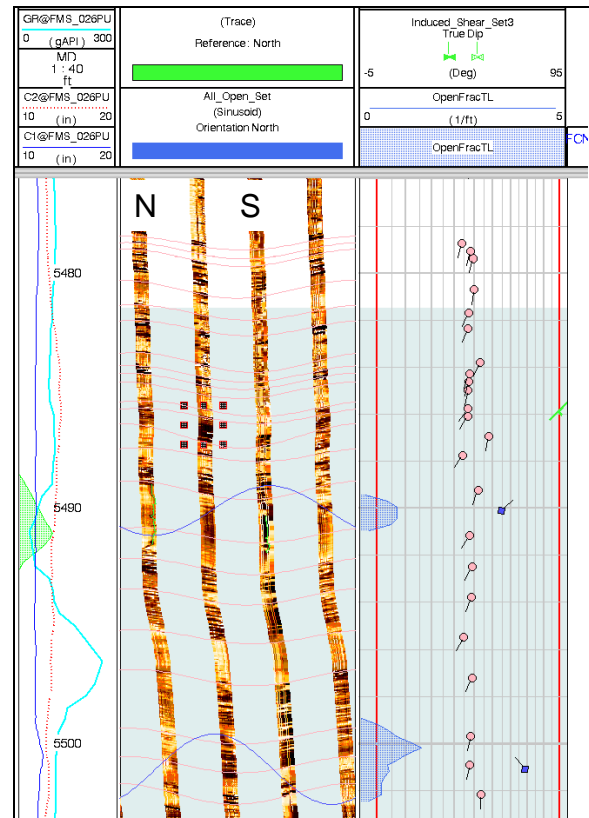


Figure 6: pre-Tertiary unit 2 hornfels shown here from 5476-550'. Figure conventions again as described in Figure 3. Note the regular foliation planes in the hornfels dipping to the southwest at approximately 30-40° dip magnitude. Note also present are drilling induced tensile fractures traced in green.

DRILLING INDUCED FRACTURE ANALYSIS

Drilling induced fractures are present at least intermittently throughout the FMI-imaged interval (Figures 3, 6, & 7). Both drilling induced tensile and shear fractures according to the classifications described by Bratton et al. (1999) are present. The drilling induced tensile fractures suggest that the average maximum horizontal stress orientation over the entire study interval is N29° (striking NE-SW), although variety does exist within the logged interval. Borehole breakouts or washouts are minimally apparent on the FMI logs. However, the poor degree of borehole coverage could mean that they are

present on the portion of the borehole wall not seen by the tool.

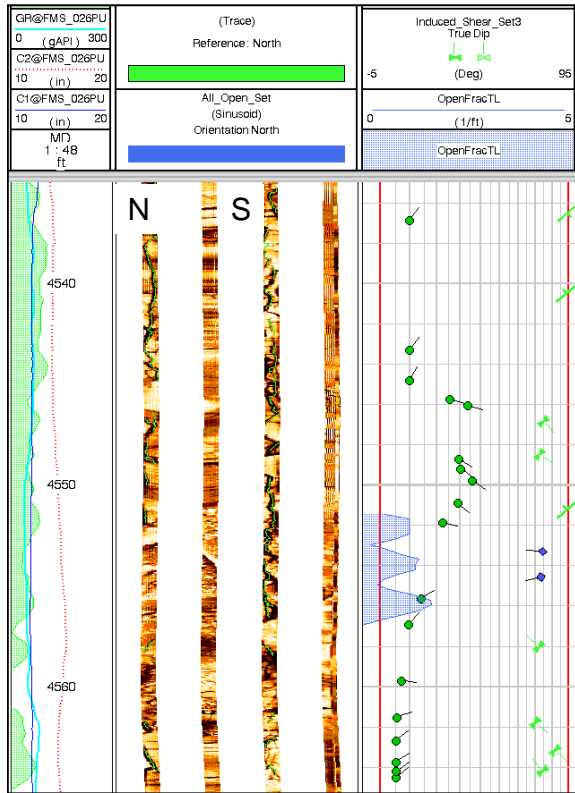


Figure 7: FMS* image from 4545-4565'. Figure conventions are as described in Figure 3. Note the presence of drilling induced tensile and shear fractures as traced on the image log. Green strike symbols show the dip magnitudes and orientations for the tensile induced fractures, and green bow-tie symbols for the shear induced fractures. Note that here all are striking NE-SW. Green area shading shown in the leftmost column calls out areas of intense drilling induced fracturing.

NATURAL FRACTURE ANALYSIS

Both open and healed (mineralized) natural fracturing is present in the studied interval of well 27-15. Healed natural fractures were less abundant than open natural fractures. More than 160 open natural fractures were identified and quantified in terms of orientation, dip magnitude, and observed trace length along the borehole path in the studied interval. Open natural fractures are sub-categorized into the following sets: partially open fractures (those that are partially mineralized along their borehole trace length) and continuous open fractures (those that are continuously open all the way around the borehole), (Figure 8). Thus, likely the continuous open

fractures by definition should be more conducive to fluid flow. For example, a continuous open fracture occurs at 4318 ft and corresponds to a localized increased caliper reading. Several populations of open natural fractures by orientation are present and dip magnitudes vary widely between 30 and 80 degrees. The largest population of natural fractures present is striking NE-SW in agreement with the near wellbore maximum horizontal stress orientation as defined by the drilling induced fractures. This fracture population has fair conjugate set development, but with more fractures dipping down to NW azimuths. Another population of fractures striking NW-SE is the second largest fracture population.

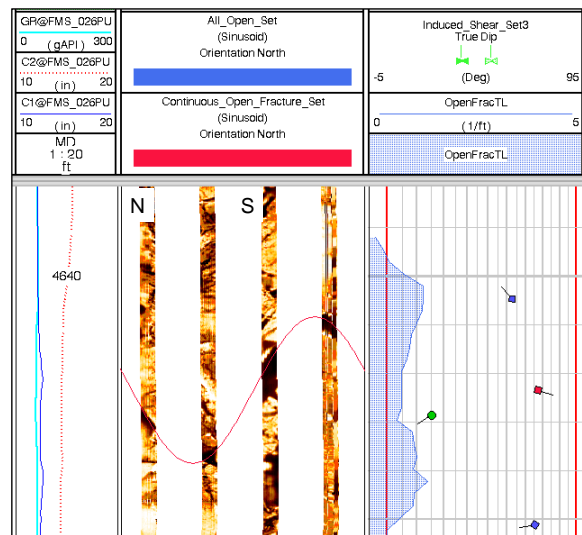


Figure 8: FMS* images from 4638-4645.5'. Figure conventions for the log as described in Figure 3. A continuous open fracture is delineated by the red sinusoid on the image in the dynamic image track. The fracture is oriented striking NE-SW, and dipping to the SE. Nearby, other partially open natural fractures are present as shown by the blue diamond symbols.

TRUE RESERVOIR FRACTURE SPACING ESTIMATION

The natural fractures identified along the wellbore path by the image interpretation process were then used to estimate true reservoir fracture spacing. Figure 9 summarizes all open fracture data for the logged interval. Schlumberger's FracView* module and workflow uses petrophysical fracture attributes and geometry including the wellbore azimuth and fracture dip and strike to generate a reservoir cross section to calculate the reservoir's effective fracture spacing by dip and strike population. An 'effective fracture' for purposes here is defined as the ratio of the hand-traced fracture as seen on the image log to

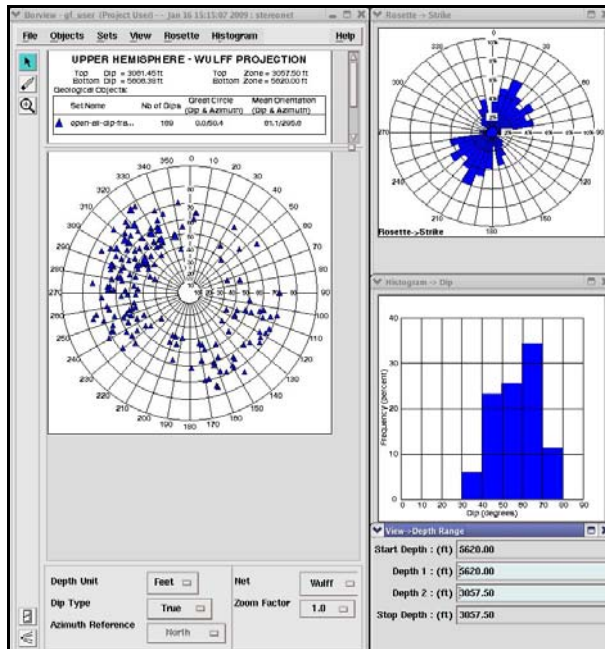


Figure 9. Summary of all open fracture data from the studied interval of well DP 27-15. The left side of the figure shows an Upper Hemisphere Wulff Projection of the data points. The upper right figure is a rosette plot summarizing fracture strike, and the lower right figure is a histogram summarizing dip magnitude.

the entire length of the sinusoid representing the fracture's planar cross-section on the borehole wall. Through these calculations, the fractures are broken out into subpopulations based on dip orientation (i.e., fractures dipping to the NE, SE, SW, etc.). For each subset, an effective statistical fracture spacing is calculated for each different zone. In this case, the logged interval was broken into 3 simple, distinct zones: 1) the Tertiary altered tuffs, 2) the pre-Tertiary Unit 1 metasedimentary sequence, and 3) the pre-Tertiary Unit 2 metamorphosed intrusives. Effective fracture densities and spacings in units of fractures per foot and feet between fractures, respectively, are calculated for each zone and over the entire interval for each fracture population (Table 1, Figure 8). Fractures dipping to the NW (striking NE-SW) were the most populous, having a statistical fracture spacing of approximately 20 ft between fractures. Each of the three zones displayed a similar spacing for this fracture population. The least abundant fracture population showed the widest range in fracture intensity in the different lithologies: fractures dipping to the NE (striking NW-SE). These fractures varied from statistical fracture spacings of one fracture per 107 feet in the altered tuffs to one fracture every 228 ft in pre-Tertiary Unit 1. This represents a difference on the order of an order of magnitude between these two fracture intensities.

Fracture spacing (in units of feet between fractures)	<u>NE</u> dip	<u>SE</u> dip	<u>SW</u> dip	<u>NW</u> dip
TERTIARY UNIT	106.7	29.9	63.4	19.1
PRE-TERTIARY UNIT 1	228.2	42.9	42.7	20.9
PRE-TERTIARY UNIT 2	149.5	40.9	61.9	21.5

Table 1. Summary of calculated statistical fracture spacing by unit for each fracture population. Units are fracture spacing in terms of number of feet between fractures. See text for discussion.

SINGLE WELL FRACTURE NETWORK MODELING

After the statistical fracture spacing within the reservoir was calculated, single well modeling efforts were initiated. In this case, as described above, the well was divided into three intervals, all containing fractures. Within each interval, the fractures were grouped into separate dip domains: NW, NE, SE, and SW. Using these statistical fracture spacings, a simple, single well fracture model was generated. Petrel* version 2008.1 software was used for modeling. The fracture spacing, expressed in feet (perpendicular to fracture orientation) between each whole effective fracture was the primary input into the Petrel* fracture modeling module.

Within each formation zone, every dip domain yields a single modeled dipset (Figure 10). Identical fracture geometry parameters were used in generating each dipset. The orientation and spacing parameters generated from the FracView* results determined the statistical orientation and frequency of fractures within the modeled volume (Figure 11). As natural fracture systems display some degree of variation in the orientation of fractures within the same dip domain, the fracture concentration variable used was one that mimicked an amount of variability commonly observed in natural fracture populations.

DISCUSSION

As noted by Lutz et al., 2009 ; Benoit et al., 1982; Lutz et al., 2004; Robertson-Tait et al., 2004, the geology of the Desert Peak area is complicated and reflects signatures of different stress regimes over time. The present-day maximum horizontal stress orientation in the near vicinity of DP 27-15 suggested by the drilling induced fractures identified in this study is generally NE-SW, in agreement with the nearby Rhyolite Ridge Fault system (Lutz et al., 2009). The largest population of natural fractures identified in this study was also oriented NE-SW, suggesting this is a fairly young fracture population, and which may be the major conduits of fluid.

CONCLUSIONS

A borehole image interpretation study of resistivity-contrast generated image logs was performed on Desert Peak study well 27-15. These findings were combined with petrologic and petrographic studies to provide a more complete understanding of the geologic characteristics of the well that might contribute to or inhibit performance of the well as an enhanced geothermal systems experiment candidate. In general, the upper Tertiary unit seems to have two subunits, the upper portion of which contains more drilling induced and natural fractures. The lower portion of this unit has few drilling induced or natural fractures and extremely irregular textures, suggesting a possible difference in reaction to stimulation. The pre-Tertiary unit 1 is composed of metasedimentary rocks displaying some variety in bedding plane orientations between subunits and may be a structurally complex unit. This rock type contains a moderate degree of drilling induced and natural fractures. Pre-Tertiary unit 2 is comprised of metamorphosed intrusives , most of which display fairly regular foliations to the SW. Natural and drilling induced fractures are present in this unit.

The drilling induced fractures present suggest a maximum horizontal stress orientation of NE-SW, consistent with the nearby Rhyolite Ridge Fault System. Several populations of natural fractures appear to be present. The largest population identified is striking NE-SW consistent with the identified maximum horizontal stress orientation and the Rhyolite Ridge Fault System. A statistical fracture spacing of approximately one fracture every 20 ft seems to be consistent through each of the major lithologic units, suggesting this is a young fracture population. Modeling was used to better visualize the fracture populations identified and characterized in this study.

REFERENCES

- Benoit, W.R., Hiner, J.E., and Forest, R.T. (1982), 'Discovery and geology of the Desert Peak geothermal field: A case history,' *Nevada Bureau of Mines and Geology Bulletin*, **Vol. 97**, p. 82
- Bratton, T., T. Bornemann, Q. Li, D. Plumb, and J. Rasmus (1999), "Logging-while-drilling images for geomechanical, geological and petrophysical interpretations," *SPWLA 40th Annual Logging Symposium*, **Paper JJJ**
- Davatzes, N., and Hickman, S., 2009, Fractures, stress, and fluid flow prior to stimulation of Well 27-15, Desert Peak, Nevada, EGS Project: Proceedings, Thirty-Fourth Workshop on Geothermal Reservoir Engineering Stanford University, Stanford, California, February 9-11, 2009
SGP-TR-187
- Faulds, J.E., Garside, L., Johnson, G., Muehlberg, J., and Oppliger, G.L. (2002), "Geologic setting and preliminary analysis of the Desert Peak – Brady geothermal field, western Nevada," *Transactions Geothermal Resource Council*, **Vol. 26**, p. 491-494.
- Lutz, S.J., A. Schriener Jr., D. Schochet and A. Robertson-Tait (2003), "Geologic characterization of pre-Tertiary rocks at the Desert Peak East EGS project site, Churchill County, Nevada," *Transactions, Geothermal Resources Council*, **Vol. 27**, p. 865-870.
- Lutz, S.J., Robertson-Tait, A., and Morris, C.L. (2004), "Stratigraphic relationships in Mesozoic basement rocks at the Desert Peak East EGS area, Nevada," *Proceedings, Twenty-Ninth Workshop on Geothermal Reservoir Engineering Stanford University*, Stanford, California, January 26-28, 2004
SGP-TR-175
- Robertson-Tait, A., S.J. Lutz, J. Sheridan and C.L. Morris (2004), "Selection of an interval for massive hydraulic stimulation in well DP 23 1, Desert Peak East EGS project, Nevada," *Proceedings, Twenty-Ninth Workshop on Geothermal Reservoir Engineering, Stanford University*, p. 216 – 221

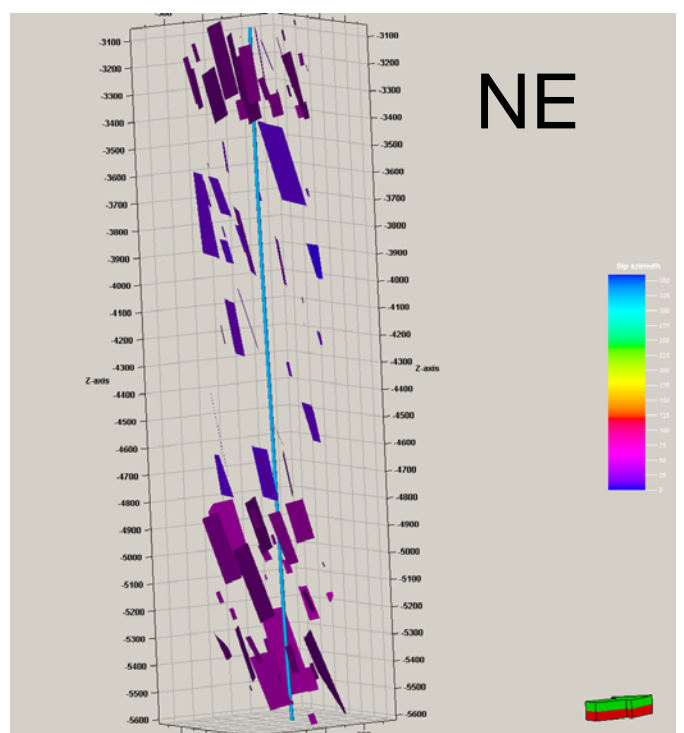
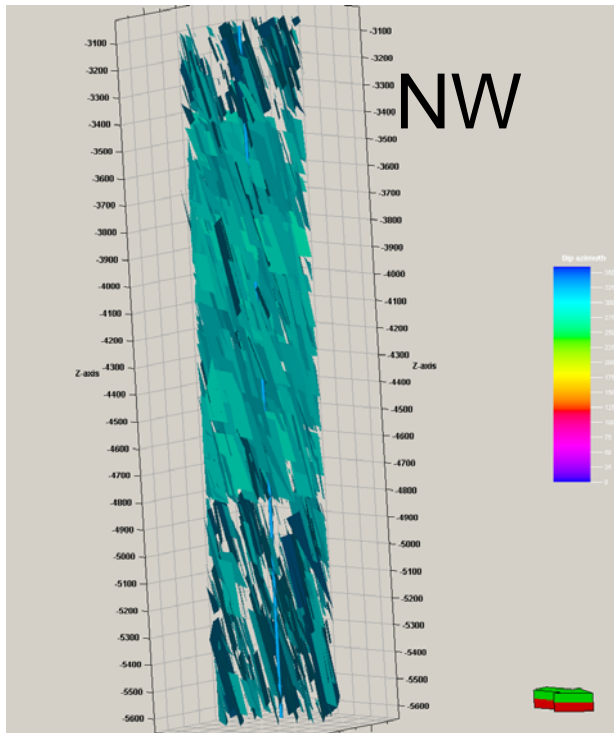
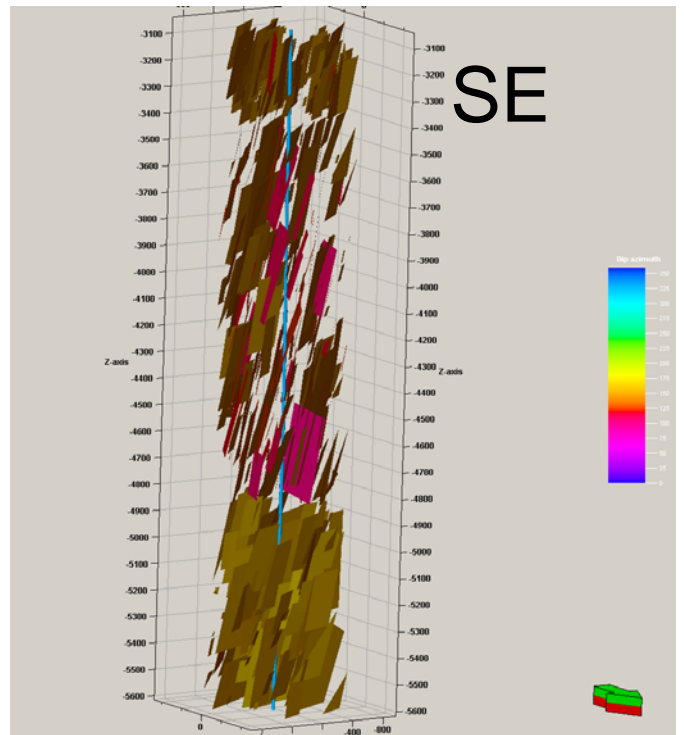
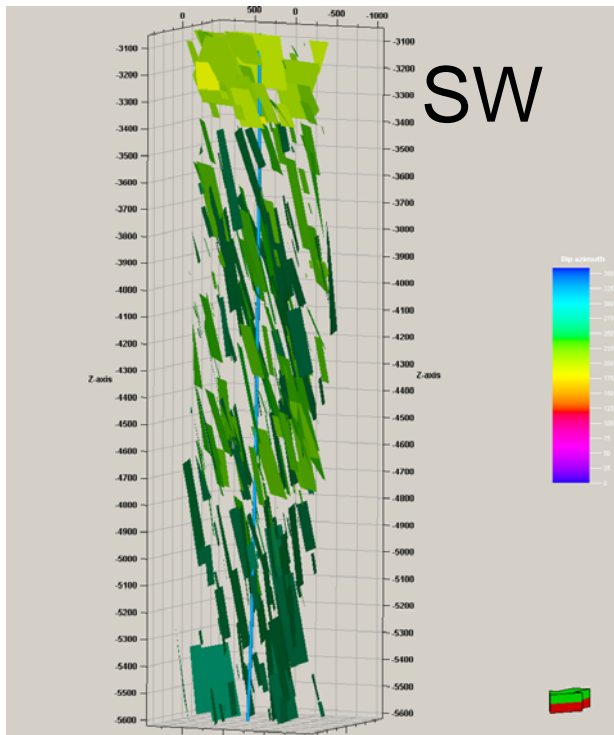


Figure 10: Single well fracture network modeling for each fracture population by orientation as described in the text. The entire logged interval is shown. The three different color shadings in each subpicture correspond from top to bottom of each picture to the Tertiary, pre-Tertiary unit 1, and pre-Tertiary unit 2 subintervals. See text for further discussion.

